Available online at www.CivileJournal.org

Civil Engineering Journal

(E-ISSN: 2476-3055; ISSN: 2676-6957)

Vol. 11, No. 08, August, 2025

Stability Analysis of Dike Pond Due to Pore-Water Pressure Changes

P. A. Maha Agung [1], Muhammad Fathur Rouf Hasan [2, 3*], Denny Yatmadi [1], Adi Susilo [3, 4], Sutikno [1], Dominggus Benyamin Osa [5], Aldo W. Adinegara [6], Mohd Adib Mohammad Razi [7], Mustaffa A. Ahmad [7], Adnan Zainorabidin [7]

[1] *Department of Civil Engineering, Politeknik Negeri Jakarta, Depok, 16425, Indonesia.*

[2] *Graduate School, Universitas Brawijaya, Malang, 65145, Indonesia.*

[3] *Center Study on Geosciences and Hazard Mitigation, Universitas Brawijaya, Malang, 65145, Indonesia.*

[4] *Department of Physic, Universitas Brawijaya, Malang, 65145, Indonesia.*

[5] *Faculty of Animal Husbandry, Marine and Fisheries Science, Nusa Cendana University, Kupang, 85228, Indonesia.*

[6] *Tenka Global Indonesia, Bekasi, 17530, Indonesia.*

[7] *Faculty of Civil Engineering and Built Environment, University Tun Hussein Onn Malaysia, Johor, 86400, Malaysia.*

Received 17 November 2024; Revised 04 June 2025; Accepted 16 June 2025; Published 01 August 2025

Abstract

The Brigif retention pond not only serves to temporarily store rainwater for groundwater reserving but also reduces the risk of flooding in the Southern Jakarta area. Research was purposed to study two critical conditions of a dike made from clayey material from before to after water impounding stages correlating with its stability. The research will investigate pore-water pressure (u) parameter changes at any stage in both conditions. The parameter of *(u)* can be predicted *(*u_{pre}*)* using the laboratory consolidation or oedometer test and measured *(*u_{act}*)* completely with hydrostatic pressure *(*u_0*)* directly in the field. Actual measurements using a piezometer were also conducted on the body of the dike. The prediction analysis used the self-developed program and conventional geotechnical software. The critical peak depth of *(u)* was found at 3.0 to 4.0 m. The actual settlement potential values reached -0.10 to -1.42 m and matched the prediction result. Safety factor *(SF)* was around 2.0 to 4.0, or in stable condition. Research results found that the magnitude parameter of *(u)* could be influenced by groundwater flow and porosity or void ratio fluctuations. The consolidation process also would affect the physical soil pore, contributing to the change of *(SF)* the dike pond.

Keywords: Consolidation; Dike Pond; Hydrostatic Pressure; Pore-Water Pressure; Piezometer.

1. Introduction

A dike pond is immediately formed after excavation during reservoir or retention pond construction. The stability of the dike made at the clayey soil area must be evaluated before and after water impounding. The most critical parameter in the evaluation of the dike stability *(SF)* on clayey soil is pore-water pressure *(u)* or (PWP). Changes in *(SF)*) of the dike can be investigated by the fluctuation of pore-water pressure. However, PWP will depend on the coefficient of permeability *(k)* [1] and the fluid flow type value of porous media in the macroscopic analysis [2]. Seepage analysis simulation should be performed before assessing slope stability analysis *(SF)*.

* Corresponding author: rouf@ub.ac.id

http://dx.doi.org/10.28991/CEJ-2025-011-08-017

Some researchers have developed research on PWP dissipation, but predicting the PWP closing to actual conditions in the field is difficult. There are errors in PWP magnitude prediction due to many factors that must be studied and explored continuously through more detailed research [3]. The dike surrounding the retention pond or reservoir area will collapse due to several mistakes undetected in prediction analysis, especially after excavation works or prior water impounding. It must be acknowledged that the classical theory does not cover all aspects that influence the magnitude of PWP in the prediction analysis. In classical theory, Darcy (1856) developed fluid flow mechanics in porous media, such as groundwater flow, using permeability analysis. Then, the prediction of PWP analysis was developed by Terzaghi (1923) using the Darcy theory and the conventional consolidation or oedometer test in laboratory work. Currently, there are many evaluations of the stability of dikes performed by researchers using the prediction of PWP parameters through oedometer test results and validated directly by the actual measurement in the field (e.g., piezometer instrumentation, piezocone (CPTU), etc.). They adopted several methods from previous research in predicting PWP using the numerical/mathematical/neural networks analysis and/or laboratory/field measurement model analysis (e.g., Cam-clay model, during pile driving, etc.). It is not uncommon for other researchers to try to compare the PWP between prediction using the consolidation in one dimension (1-D) and actual measurement results without considering the pre-consolidation pressure (σ'_p), where there are 3 (three) conditions, such as normal $(\sigma'_p = \sigma_{vo})$ (NC); over-consolidated $(\sigma'_p > \sigma_{vo})$ (OC) conditions; and transition of both conditions or under-consolidation [4, 5]. However, their prediction of PWP results differed significantly between the laboratory and/or the field investigations. They do not infrequently ignore these problems without an accurate explanation, resulting in the dike collapse during the service period and causing considerable flooding around the retention pond. The most recent research mentioned that evolution causes these differences in changes from microstructure and some mistakes when inputting macroscopic parameters into the equations of the time rate of consolidation. The PWP and (*k*) parameters during the consolidation incremental loadings of clayey soil layers will change in 3 (three) stages: natural structural, restructuring, and slight change. It is essential to study the consolidation characteristics of soft clay based on the three stages in determining the pore-water pressure [6, 7].

The research aims to investigate pore-water pressure (u) parameter changes at any stage of both these conditions. This paper will study the prediction of PWP change during the loading and/or unloading process before and after water impounding the reservoir. Conditions of NC and/or OC will be considered. The type of groundwater flow mechanically in soil pores will be assessed in both conditions as the principle of continuity of flow at the soil element in classical theory. However, manual continuity principles analysis can be complicated and time-consuming, especially for complex dynamic fluid systems. Besides that, due to the highly complex nature of the phenomena involved in correlations between the PWP and the (k) parameter, many fundamental questions remain unanswered or are still lacking. For this case, soil investigation for NC data at laboratory works was unavailable, or this test was not performed during the design work at the beginning of the project. Thus, this study is only concerned with the transition of NC to OC or under-consolidated conditions influencing the PWP. With some limitations of this research, the self-developed program will define the determination of PWP magnitude to resolve the numerical analysis (e.g., derivation and solution of Terzaghi's one-dimensional (1-D) theory for one and double layers using the laboratory consolidation data results and seepage analysis simulation (Seep/W)). Parameters of (k) parameters are determined by the correlation cone and/or standard penetrations (CPT, SPT) [8]. Validation of these results will be compared to the actual measurement from piezometer investigation in the field before and after water impounding. The validation of the appropriate or true interpretation of PWP can yield the specific information for the stability analysis (Slope/W) based on the fluid flow pattern of groundwater in determining *(SF)*. Here, some input parameters of cohesion (c) and internal shear angle (φ) are derived by the simulation of effective stress (σ'_{vo}). Hereinafter, validation of the results can be compared directly in the field through observation works, such as cracking and/or erosion problems, horizontal movements, etc. [9].

2. Methodology

2.1. Research Stages

Generally, research activity will be started to collect all secondary databases that can be used in the geotechnical analysis, such as the previous field and laboratory data during the design works, topography map, hydraulics of surface and model of groundwater flow map, the elevation of groundwater, rainfall data, etc. [10]. Qualitative results of previous research were also collected, including geology maps and environment studies [11]. The consolidation laboratory obtains primary data for implementing the macroscopic method using undisturbed samples (UDS) from 6.0 and 10.0 m depths. Prediction works of PWP $(u_{(per)})$ will be validated by direct observation through actual measurement of piezometer instrumentation $(u_{(act)})$ at a similar depth. The research flowchart is shown in Figure 1.

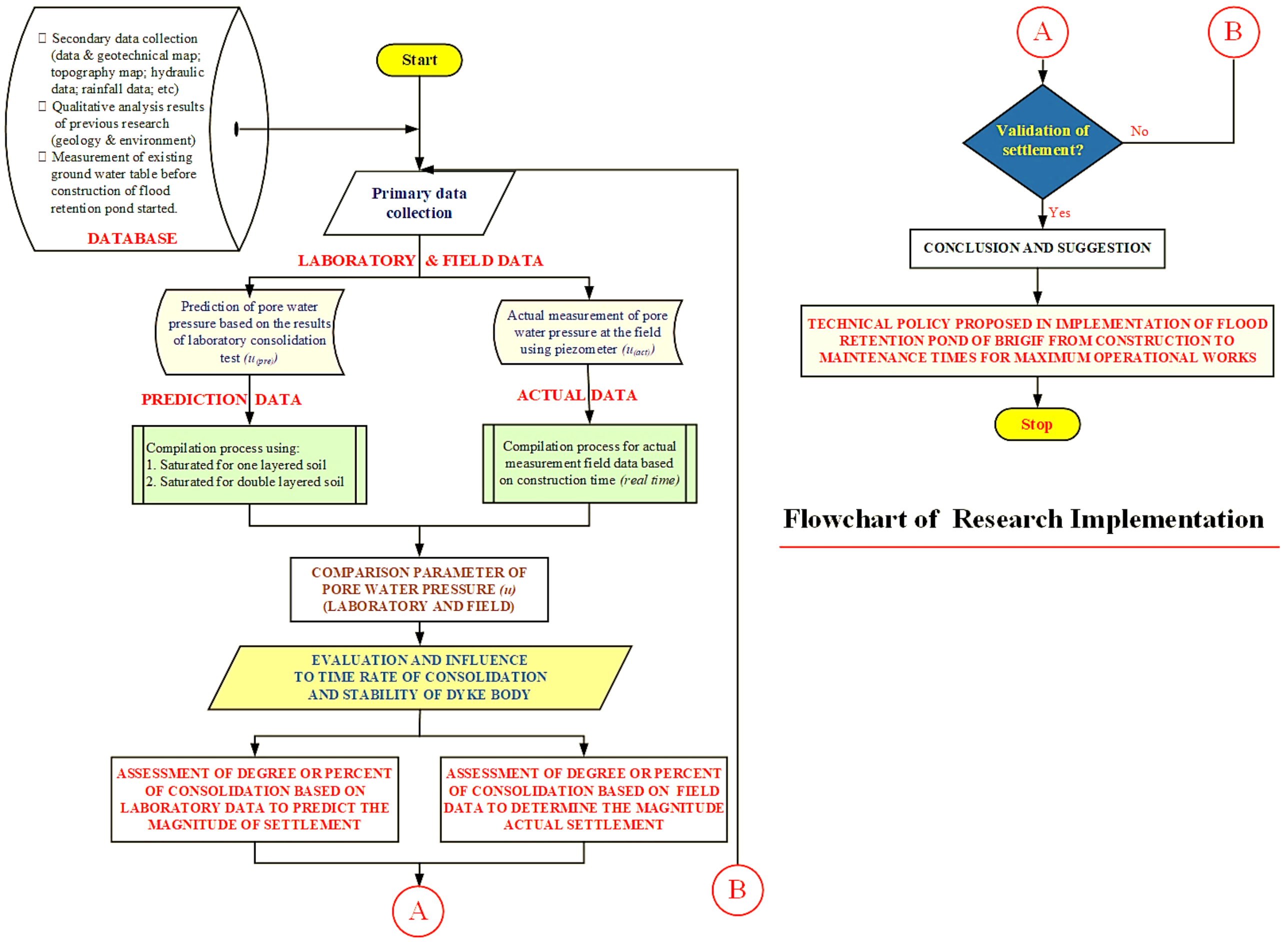

Figure 1. Flowchart for all activities of the research

All UDS samples for laboratory consolidation or oedometer test will be taken from the existing dike body surrounding the reservoir area. These consolidation data results will be used for prediction analysis of PWP ($u_{(pre)}$) using saturated one and double-layer soil of one dimensional (1-D) theory using numerical analysis with software from EMACS; FORTRAN COMPILER 8.1 and GNUPLOT 4.0 and standard software from GEOSTUDIO (Seep/W).

The time rate of consolidation will be assessed during simulations for all analysis steps. The magnitude of PWP as the function of the degree of consolidation from primary consolidation data results is simulated continuously until close to the actual measurement at the field. These steps are taken because, in theoretical and experimental works, the fluid flow which correlates to PWP is typically attempted to find functional correlations between the *(k)* parameter and some other macroscopic properties of the porosity and the specific surface areas [12]. This simulation is to avoid the complexity analysis of the actual microscopic flow paths through the soil pores. Finally, all PWP data are applied in the computer software simulation (Slope/W) to determine the *(SF)*.

2.2. Study Area

The research study is located at the Brigif flood retention pond or flood water reservoir development project, Cempedak Village, Jagakarsa District, Southern Jakarta City, Java Island of Indonesia, as shown in Figure 2. This project intends to temporarily accommodate flood discharge from the southern region (Bogor and Puncak areas in West Java) through the Krukut River before the flow enters Jakarta's southern area's natural and/or artificial drainage system. The project Brigif retention pond is divided into two parts, namely the upper and lower reservoir areas. Upper and lower areas have 3.3 and 6.7 Ha with 104.000 m^3 of volume capacity and 152.000 m^3, respectively.

Regional topography is a basin area in Southern Jakarta City of Indonesia, with the elevation of a low hilly terrain area of 50 to 140 m above mean sea level (MSL) and a slope gradient of less than 15%. In geographic situation, the research area exists on Aselih Street, bordered on the north by the South Jakarta area, to the south by the Cipedak Sub-district, to the east by Gandul Village, and to the west by Ciganjur District. The Brigif flood retention pond region is a tropical climate, and rainfall data at several stations indicates that the precipitation volume is 1 to 591 mm, with the number of rainy days between 10 - 20 days. During the rainy season, the average monthly rainfall is around 327 mm, and the maximum flood discharge of the Krukut River track can disturb the stability of the dike pond [13].

Figure 2. Study location of prediction and actual measurements of pore-water pressure *(u)*

2.3. Geological Aspects

A geological point of view is used to predict the soil layers due to the weathering of existing rock layers. Generally, exposed clayey layers to a depth of 12.0 m can be found easily near the Krukut River. Based on the Geological Map of Jakarta and Kepulauan Seribu Quadrangles as shown in Figure 3 [14]. The Brigif reservoir in southern Jakarta could be classified into 2 (two) rock formations: Alluvial (Qa) and Alluvial Fan (Qav). The stratigraphy of the research area in the Alluvial Formation (Qa) is composed of clay, silt, sand, gravel, pebbles, and boulders. While the Alluvial Fan Formation (Qav) is composed of bedded fine tuff, sandy tuff, and interbedded conglomeratic tuff. At these formations, PWP, or *(u)* was influenced by the *(k)* parameter. As weathering geologically results from geologic formation [15], the soil layers have various permeabilities [16]. It can be indicated that a significant permeability *(k)* at the base of the dike body could be shown for the finely layered tuff, sandy tuff interspersed with conglomerate [17]. Generally, exposed clayey layers to a depth of 12.0 m can be found easily as long as the Krukut River; these zones are susceptible to changes in PWP [18].

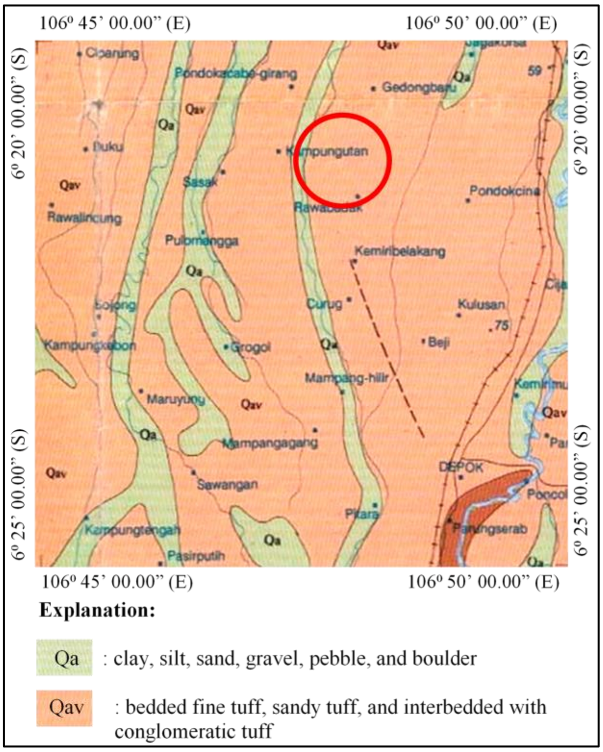

Figure 3. Geological Map of Jakarta and Kepulauan Seribu Quadrangles (Modified) [7]

2.4. Geotechnical Aspects

After geotechnical data is validated by the geological map, as shown in Figure 3, Secondary data consists of geotechnical data (laboratory data of physical-mechanical properties including the oedometer test data; field data of CPT and SPT) before the project implementation completed with topography map, geological map, previous studies of existing environment and surface-ground water hydraulic aspects, rainfall or precipitation data, etc. The soil layer and parameter of *(k)* were arranged by correlation between (CPT) and (SPT) to the depth of 15.0 m [19, 20]. The field investigation results helped determine soil layers, unsaturated & saturated weight volume *(g)* [21], cohesion *(c)*, internal friction angle (*f*), etc, through parameter correlations [22]. The shear strength parameter consists of (c) and (f) parameters, which can be obtained by laboratory direct shear or triaxial tests. The methods from Simplified Bishop, Janbu, Spencer, and Limit Equilibrium will be applied in the slope stability analysis because the effect of PWP is seriously considered [23].

2.5. Prediction Measurement of Pore-Water Pressure

Classical theory in evaluating the PWP *(u)* and permeability *(k)* using the laboratory consolidation will produce deformation due to alteration of soil volume [24]. If the soil is saturated, changes in volume cause water to come out of the pores based on consolidation theory from Terzaghi (1923) and fluid flow theory from Darcy (1856) for one and double-layered clayey soil [25]. The permeability *(k)* of soft soil and clayey layers in the study area is minimal, and the groundwater flow can last long without drainage (undrained condition). Schematically, this charge without water flow causes an increase in PWP or *(u)*, which returns to hydrostatic pore-water pressure conditions over time *(t)* [26]. Furthermore, the pore-water pressure can be interpreted as a normally consolidated and/ or over-consolidated condition as long as the prediction analysis [27]. During the consolidation process at the laboratory, one dimensional (1-D) for predicting the pore-water pressure in saturated one-layered $(u_{(pre)})$ soil can be predicted by Equation 1:

$$c_v \frac{\partial^2 u}{\partial z^2} = \frac{\partial u}{\partial t} \tag{1}$$

The response of the pore pressure $((u_{(pre)})$ to groundwater fluctuations in saturated double-layered (1-D) soil can be calculated by the Equation 2 [28]:

$$c_{vi} \frac{\partial^2 u_i}{\partial z^2} = \frac{\partial u_i}{\partial t} \ (i = 1, 2) \tag{2}$$

Both these interpretations are shown in Figure 4. The coefficient of swelling or consolidation (c_v) typically contains the material properties that govern the consolidation process. This parameter has dimensions of L^2T^{-1} in m^2/second unit. Then, $(u_{(pre)})$ is a function of both the space or depth variable in the soil element *(z)* and the time of consolidation *(t)*.

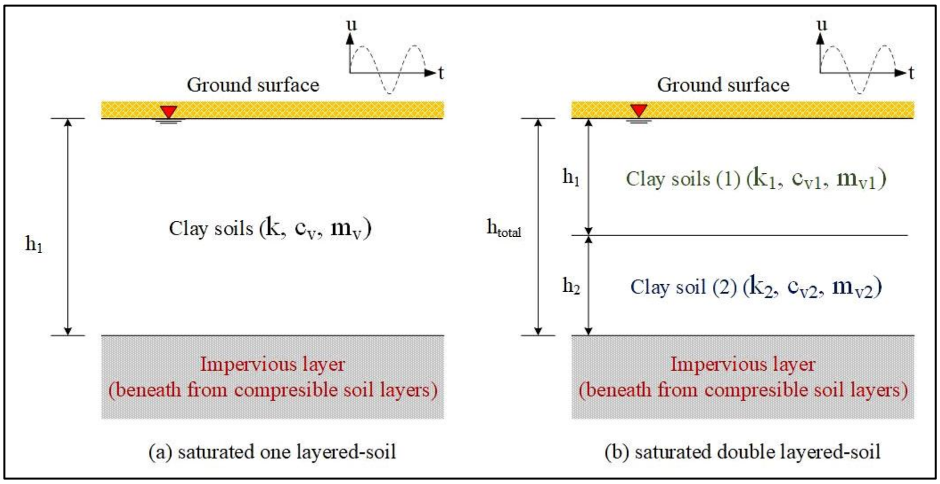

Figure 4. 1-D consolidation model for saturated soil in one and double-layer (after modification) [28]

The consolidation data for $(u_{(pre)})$ was compiled at the consolidation laboratory following the standard from ASTM D 2435-04 [29]. Independent variable consists of initial (R_o) and final (R_n) data reading according to time consolidation (n = 1,2, … and magnitude of settlement $(s_{(t)})$ from dial gauge during testing. The dependent variable would cover initial and modified secondary index compression (C_a and C_{ae}); coefficient of consolidation (c_v); length of drainage path; average degree or percent of consolidation $(U_{avg}$ *or U)*; consolidation ratio (U_z); depth and time factor ($f_1 (Z)$ and $f_2 (T)$), respectively; stress and/or loading increment (Δs or $(\sigma'_2 - \sigma'_1)$); and permeability coefficient *(k)* [30, 31] for saturated one-layered. For saturated double-layered (1-D) or the PWP at the upper boundary, the equation governs the generation and propagation of excess PWP in clayey soil layers. Both boundaries for one and double-layer used the previous layers at the upper and lower of the clayey layers. There is no difference in analysis between one and double layers, as shown in Figure 4; the only difference is the number of compressed layers during the consolidation process [32]. The change in the PWP distribution due to changes in water level affects the strength of the soil, which involves the stability of the dike [33]. Ensuring the *(SF)* of the dike pond is of great significance in the study area. Seepage failure and other failures associated with seepage are the primary forms of failures in the dike engineering design during the flood period [34].

2.6. Actual Measurement of Pore-Water Pressure

A piezometer is a geotechnical sensor instrument used to measure PWP in the soil. Implementation of instrumentation devices and actual measurement at the field is shown in Figure 5, and Equation (3) is intended as the formula or Equation for converting a height of liquid in the piezometer column from milliampere (mA) to mH_2O:

$$u_{(act)} = \frac{(H - 4.0609)}{0.0159362} \,.\, 0.1022 \tag{3}$$

Piezometer measurement using Indonesia regulation or standard (SNI) [35, 36] ($u_{(act)}$) directly at the field would record temperature, data reading at depth 6.0 and 10.0 m, real-time data, and groundwater table elevation as the independent variables. Digital data on pore-water pressure ($u_{(act)}$) will be used as the dependent variable [37].

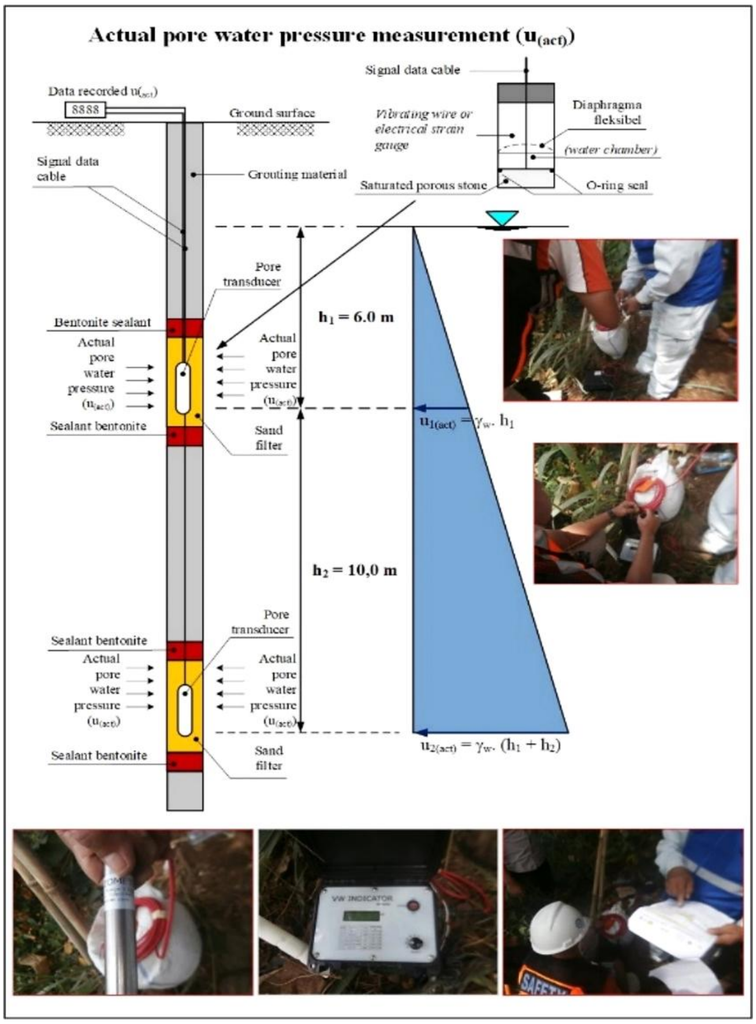

Figure 5. Instrumentation of Piezometer devices and implementation of actual measurement

2.7. Comparison between Prediction Analysis and Actual Measurement

Based on several references in recent years in previous literature reviews, excess of PWP at any time *(t)* according to the alteration loading, this function of depth *(z)* and time *(t)* will vary from one point to another as an isochrone parabolic [38, 39]. Prediction analysis at the consolidation laboratory and actual measurement in the field is very useful for monitoring shear strength and stability conditions at the dike body of a reservoir or pond. Unfortunately, during construction, sometimes all designers used field tests (SPT; CPT) where they did not complete the laboratory consolidation results data [40, 41]. Variations of low-water level (LWL) and high-water level (HWL) can be the essential reason for the change of *(SF)* values of the dike surrounding the reservoir due to the changes in PWP. In this case, stability analysis is performed in both conditions [42]. The other major factor influencing the dike is the settlement based on time-dependent consolidation analysis under surface loads (surcharges). The research results are used to propose the technical model related to construction and maintenance methods to the local government and to support the life service of retention ponds in avoiding and/ or managing floods in southern Jakarta. Monitoring and evaluation also involve the environment supervising the groundwater table during dry and rainy seasons [43].

3. Result and Discussion

3.1. Physical and Mechanical Soil Properties

Soil parameters were derived by correlation between cone penetration test (CPT) and standard penetration test (SPT) to the depth of 15.0 m. There were 3 (three) soil layers in the study area, shown in Table 1. Prediction analysis of PWP based on the laboratory oedometer tests was conducted for both types of analysis, such as saturated one and double-layer soils in one dimensional (1-D). One-layered type follows the soil configuration shown in Table 1, where clay and silty clay are combined into 1 (one) layer only. In comparison, the double-layered type follows Table 1, which consists of 2 (two) separate layers, namely clay and silty clay.

Table 1. Physical and mechanical properties at the dike body of Brigif retention pond

Properties of soil	Layer-1 (0 – 3.5)	Layer-2 (3.5 – 10.5)	Layer-3 (10.5 – 15.0)	Unit (m)
Classification	Clay	Silty clay	Silty sand	-
Model	Mohr – Coulomb Equation	Mohr – Coulomb Equation	Mohr – Coulomb Equation	-
Type	Undrained condition	Undrained condition	Undrained condition	-
γ_m	17	18	19	kN/m^3
γ_{sat}	19	20	21	kN/m^3
E	7,000	12,000	12,000	kN/m^2
c	12	55	5	kN/m^2
υ	0.3	0.4	0.3	-
k	1.0.e^{-05}	1.0.e^{-03}	1.0e^{-04}	m/day
f	32	32	38	°

The theory of consolidation has been discussed by many researchers [26]. Consolidation is linked to changes in effective stress *(s'_{vo})* resulting from changes in PWP. Upon application of an external or internal load in one-dimensional or (1-D), there is an increase in PWP throughout the UDS sample [44]. During excavation, when construction begins, all external load is initially transferred into excess PWP from hydrostatic pressure. Thus, there is no change in the effective stress in the clayey soil layers. Gradually, as the water is squeezed under a pressure gradient, the soil layers compress and take the load, increasing the effective stresses. Eventually, the excess of PWP from hydrostatic pressure becomes zero, or the PWP will be the same as hydrostatic pressure before loading. In ideal saturation, the soil's load is entirely borne by the water within its pores. Yet, achieving perfect saturation in practice can be challenging due to occasional inconsistencies during sample preparation. Therefore, it is not uncommon for pore water pressure (PWP) readings to fall short of the theoretical maximum, as real-world measurements often involve slight disturbances or inaccuracies [45]. In some scenarios, the observed pressure may be considerably lower—reaching only around 80% of the expected value [46].

Figure 6 shows the results of the oedometer test at the laboratory. An average of results indicated that the dike pond formed by a clayey layer has experienced the OC conditions where $\sigma'_p > \sigma'_{vo}$ [47]. These figures can explain that the soil layer formed by the dike has the change of total or effective stress that occurred during prior and after water impounding to the reservoir. Desiccation of the upper layers due to surface drying will also produce over-consolidation. Even though there is unavailable data for NC conditions, alteration condition can be stated that there is the transition condition from (NC) to (OC). At this condition, the clayey layer has not yet come to equilibrium under the weight of the overburden load, and PWP prediction would be the same and/ or to excess hydrostatic pressure. From Figure 6, these results implied that the PWP magnitude from NC specimens would be greater magnitudes than OC specimens [48]. In another research study using the piezocone field test (PCPT), some researcher found that the PWP be low or even negative due to their dilative behaviour in (OC) soils (with OCR > 1) in OC soils is positive regardless of OCR value. However, due to the limited understanding of these phenomena in OC soils, reliable prediction of initial pore pressure for the theoretical interpretation of dissipation tests and real-time evaluation of hydraulic properties of OC soils from PCPT has been challenging [49]. The findings of these studies could explain a complicated multi-physics problem because it would require the accuracy of specialized techniques in estimating the *(k)* parameter of soils [50].

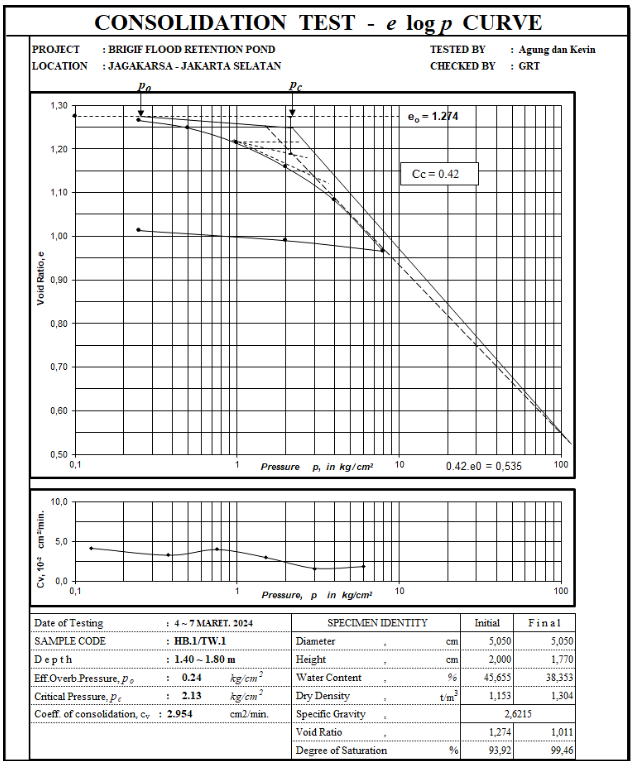

a. Point No. 1 (TPC-1) for test 1

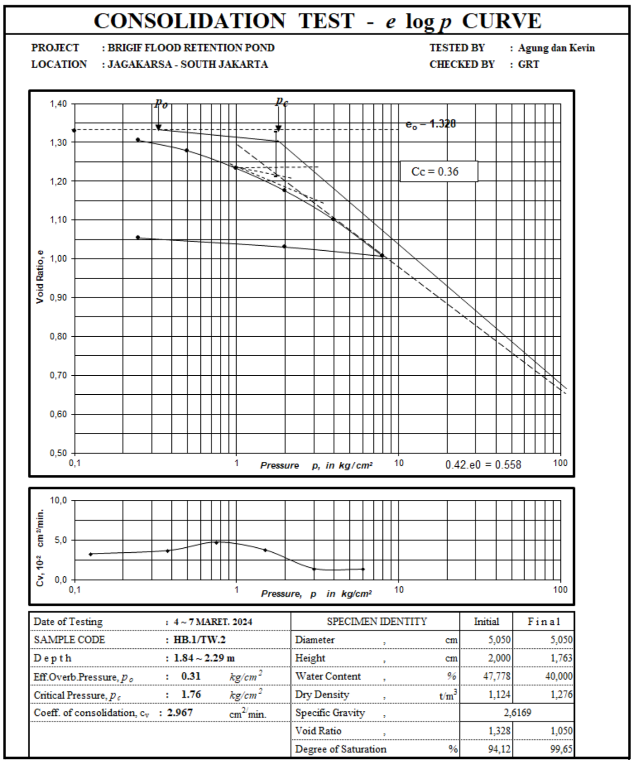

b. Point No. 1 (TPC-1) for test 2

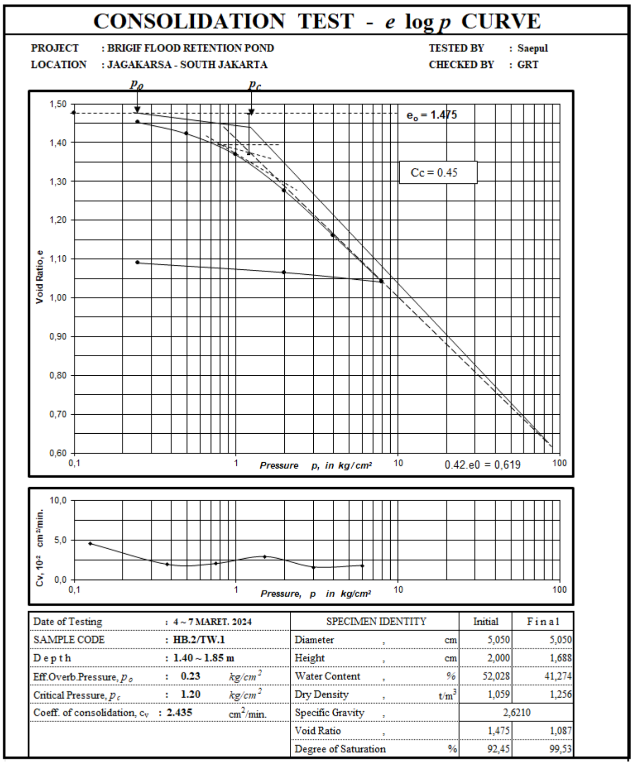

c. Point No. 2 (TPC-2) for test 1

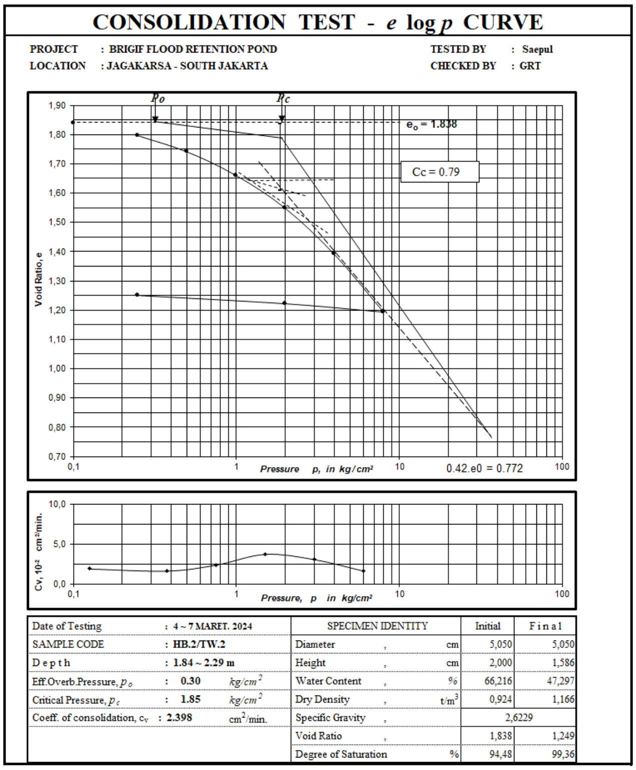

d. Point No. 2 (TPC-2) for test 2

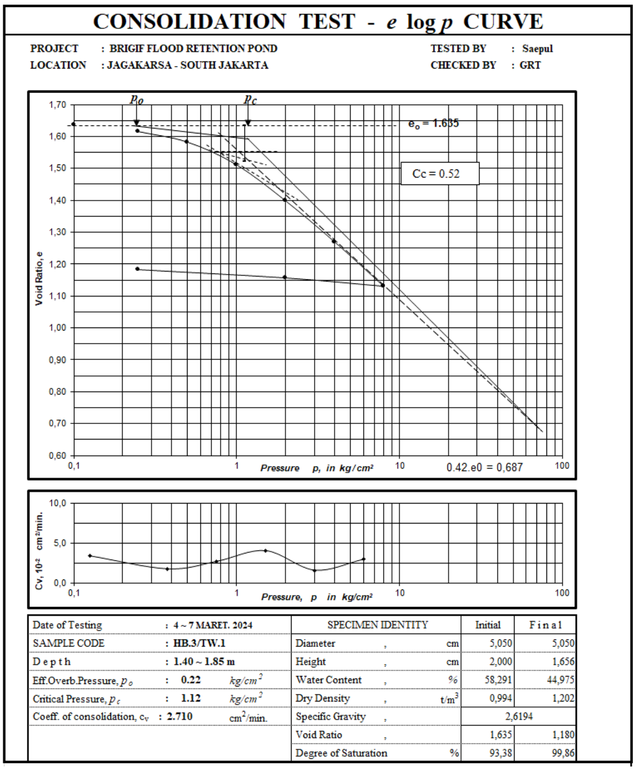

e. Point No. 3 (TPC-3) for test 1

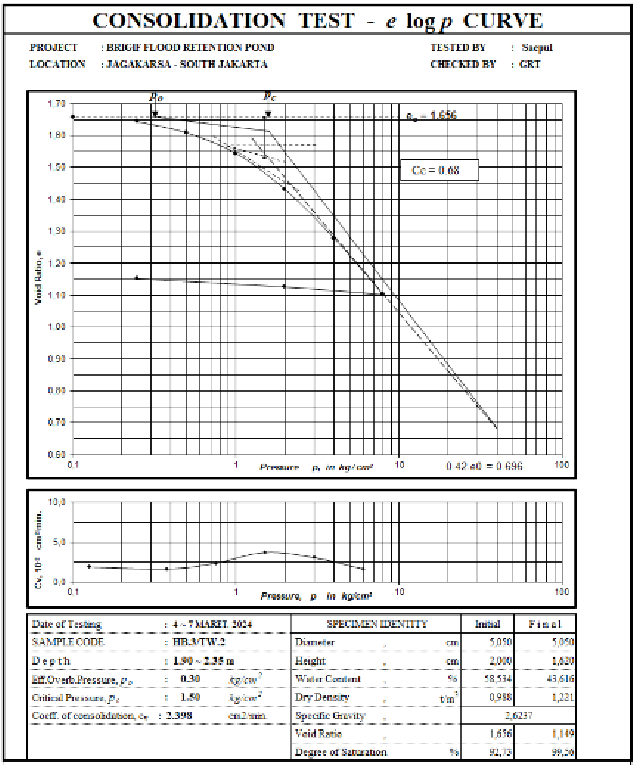

f. Point No. 3 (TPC-3) for test 2

Figure 6. Typical laboratory consolidation test results during impounding water

When an external load is applied to a saturated soil sample, it exhibits a distinct response. Based on oedometer testing principles, this load initially causes a sharp rise in pore water pressure (PWP) within the soil. The transfer of total stress to the pore fluid occurs in two clear phases. The first phase is marked by a rapid and substantial increase in PWP, reflecting most of the imposed load. Following this, the pressure rises more slowly and incrementally until it reaches its maximum level. Once that peak is attained, the pore pressure dissipates over time [51].

3.2. Prediction of Pore Water Pressure During Water Impounding

The result of the prediction of PWP based on the oedometer data using saturated one and double-layer in one-dimensional (1-D) analysis can be shown in Figure 7. The results were derived from the Equations 1 and 2 by numerical analysis. During numerical analysis, as the one-dimensional consolidation problem requires a variation of initial boundary conditions, loading histories, and soil layer thickness, the calculation process will take quite a long time and often result in multiple errors. As with single-layer systems, dimensionless parameters are critical in developing pore water pressure in saturated double-layered soils. The magnitude and depth affected by excess pore pressure are inversely related to phase shift and amplitude reduction. Additionally, differences in relative permeability between the two clay layers—or between two homogeneous clay soils—can lead to distinct pore pressure responses in each layer.

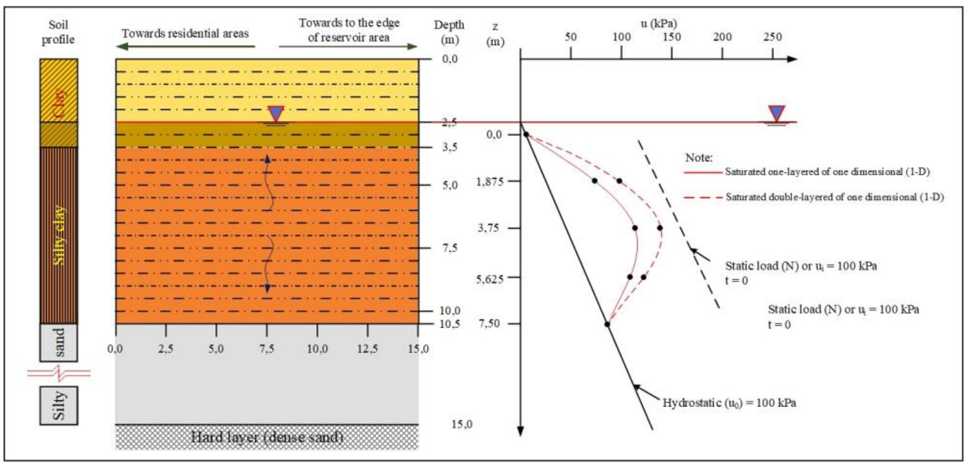

Figure 7. Excess pore-water pressure (by numerical analysis) exists above the hydrostatic water pressure

The difference in the results of the analyses was more implied by some unknown factors, such as the dimensionless parameter of relative (k) ratio of two clayey, degree of soil consolidation, variation of soil layer thickness, etc. In the study parametric in macroscopic, in single-layer soil, the influence of the coefficients of permeability and compressibility of soil on PWP distribution is different. It cannot be combined into the coefficient of consolidation of the soil in double-layered soil. In practical math processing, the various results are due to the iteration process to achieve analytical solutions in a self-developed program. Changes in input data of total weight volume and/ or the saturated weight volume and the depth of groundwater of alteration dimensionless parameters, the permeability and the compressibility in typically and/or over-consolidated conditions make it difficult to reset these parameters at the beginning of the analysis. Generally, the results indicated that it should dissipate slowly once the maximum pressure value has been reached. In the OC condition, hydrostatic pressure may be started by the negative of PWP, and then, the PWP reaches the specific point of peak of PWP and decreases gradually after sometime during the transition condition from (NC) to slightly (OC) at the over-consolidation ratio (OCR) < 4.0. The peak of PWP occurred at a depth of. 3.75 m (or 3.0 to 4.0 m), PWP will close to hydrostatic pressure *(u_o)* according to the additional depth. It can be implied that larger pores were much compressed under lower consolidation pressure, and small pores would be increased.

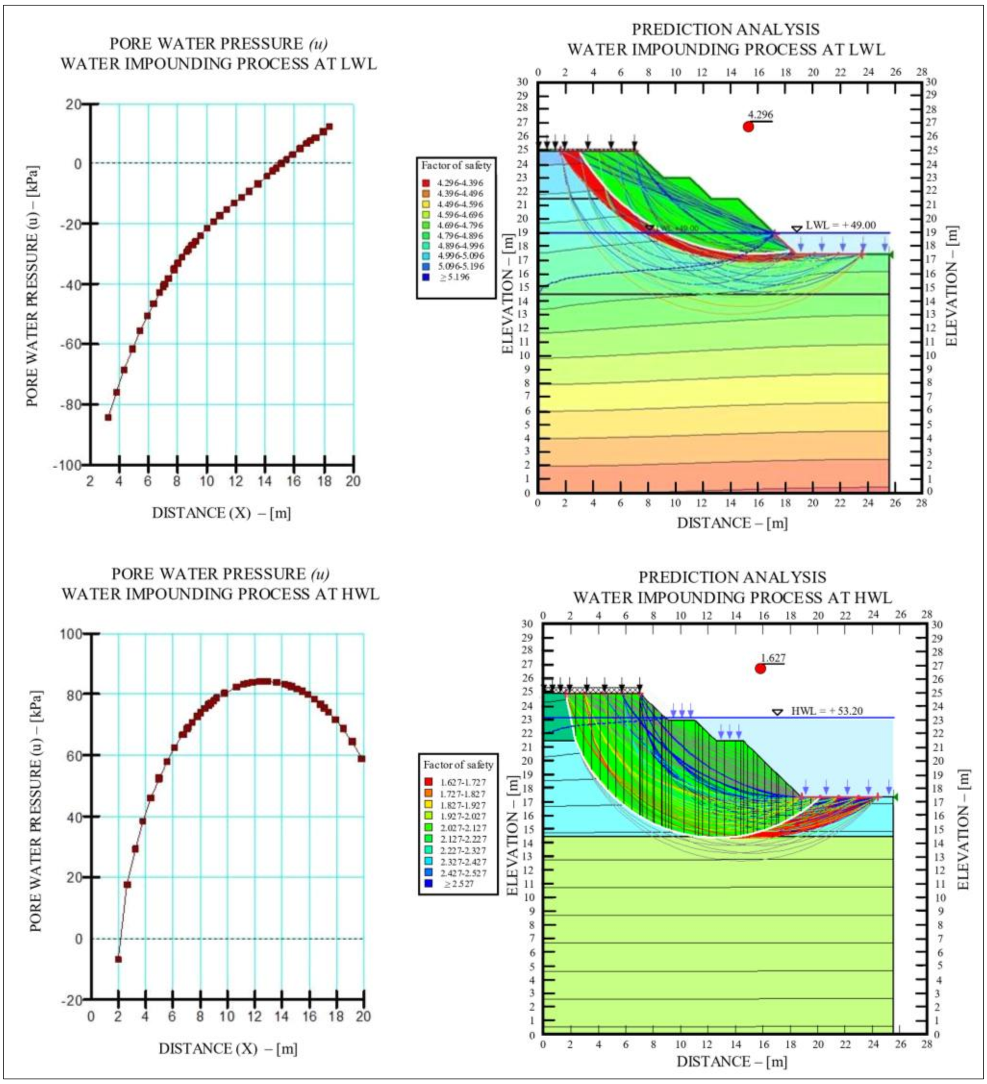

Figure 8. The typical pattern of pore-water pressure at the dike body indicates NC and OC conditions

Pore water pressure prediction was also assessed by the seepage analysis of the finite element method (Seep/W & Slope/W), as shown in Figure 8. Using this analysis, all soil parameter data from the cone and standard penetration tests were on these simulations. This study parametric involved 2 (two) conditions, such as low-water level (LWL) and high-water level (HWL) in static conditions. The typical pattern of PWP at low-water level (LWL) and/ or high-water level (HWL) is shown in Figure 8. The pattern of pore-water pressure indicated over-consolidated (OC) conditions [47]. There are many well-documented studies on the magnitude of PWP by several researchers. The results from the simulation show that the initial PWP *(u_0)* is the difference between (LWL) and (HWL) conditions, but both magnitudes have negative values. It can be implied that this difference of *(u_0)* is due to the fluctuation of the groundwater table and the estimation of slight drawdown conditions.

The results from the finite element can imply that the fissured and/or desiccated crustal layer occurred in soft to firm clayey soil at the dike body for transition conditions ((NC) to (OC)). Condition of (OC) must be warranted if the presence or lack of fissuring is not known a priori, then blind adoption of a correction can be imprudent since the correction may be unconservative. However, even though the initial negative PWP or (u_o) is different, PWP would increase to the peak point and decrease gradually to the hydrostatic or groundwater table pressure.

3.3. Measurement of Pore Water Pressure During Water Impounding

In this research, as shown in Figure 9, a piezometer standpipe was used to measure the pore-water pressure at the field directly. There are 2 (two) pore-water pressure measurements at a depth of 6.0 and 10,0 m. This measurement period was from prior excavation to the water impounding process. The average excavation height is 8.0 to 10.0 m with a slope surface length of 20.0 – 22.0 m and a slope angle of 26° to 30°. These investigations were undertaken on points No. 1 (TPC-1), No. 2 (TPC-2), and No. 3 (TPC-3) of the dike body, respectively. All conditions of the dike body were assumed that the clayey layers were already in (OC) conditions to a depth of 6.0 to 10.0 m. However, at a depth of 10.0 m of No. 2 (TPC-2), the indicated clayey layer is still in (NC) condition. The phenomena could imply that the transition condition from (NC) to (OC) would be distributed from the upper to the lower layer. The degree of consolidation values would affect the PWP dissipated to change (NC) to (OC) conditions [52].

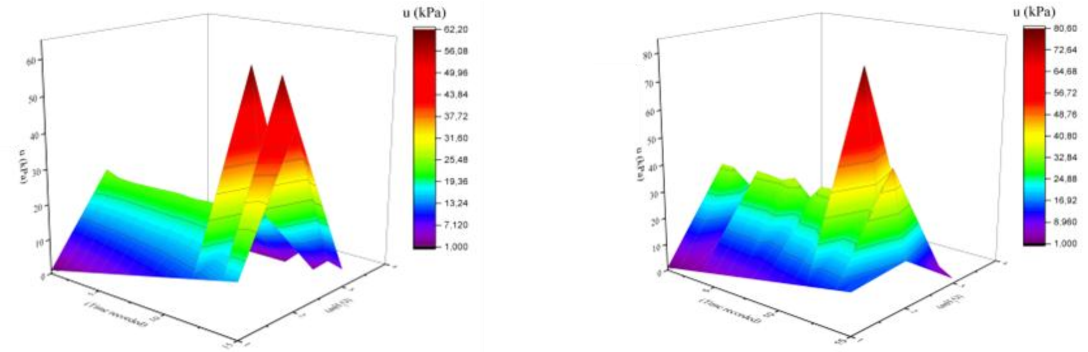

a. Piezometer No.1 (at a depth of 6.0 m) b. Piezometer No.1 (at a depth of 10.0 m)

(From January 05th to June 08th 2022)

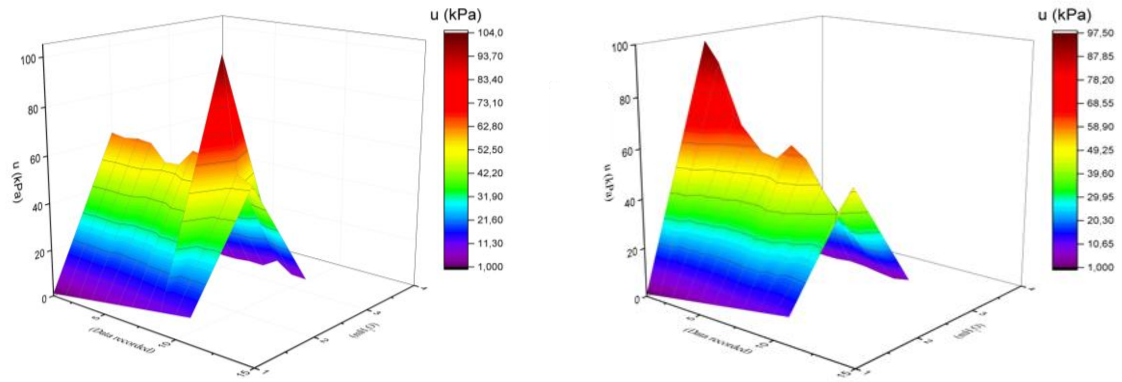

c. Piezometer No.2 (at a depth of 6.0 m) d. Piezometer No.2 (depth of 10.0 m)

(From January 05th to June 08th 2022)

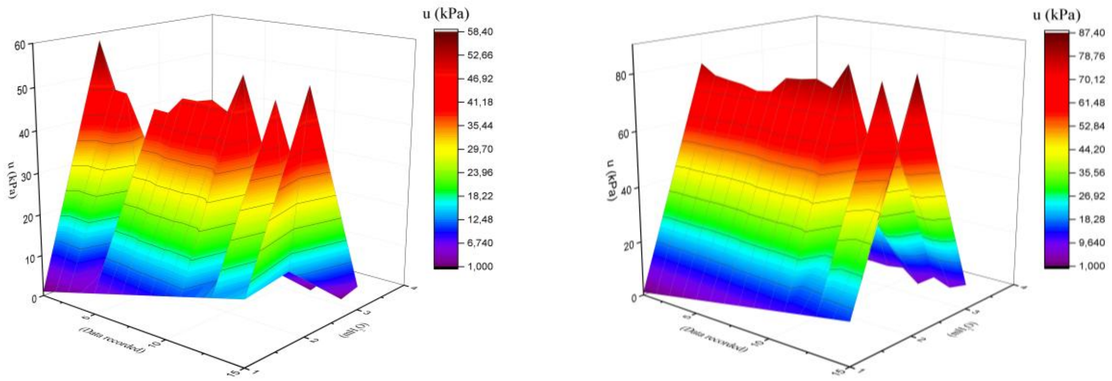

e. Piezometer No.3 (depth of 6.0 m) f. Piezometer No.3 (depth of 10.0 m)

(From January 05th to June 08th 2022)

Figure 9. The results of pore water measure measurements during the impounding of the reservoir

Pore-water pressure at Point No. 1, at a depth of 6.0 m, increased from 22.18 kPa to the peak point of 51.34 kPa after 3.0 months and returned gradually to hydrostatic pressure of 32.11 kPa after 6.0 months. With a similar observation time, at a depth of 6.0 m, it increased from 26.53 kPa to the peak point of 98.01 kPa and was stable at hydrostatic pressure of 26.90 kPa. The results of Point No. 1 were almost similar to Point No. 2 at a depth of 6.0 m. Generally, both patterns of Points 1 and 2 at a depth of 6.0 m only occurred for the (OC) condition of the clayey soil layer. However, at Point No. 3 of depth of 6.0 m, the hydrostatic pressure of 74.32 kPa would decrease to reach 67.40 kPa after 3.0 months and back to hydrostatic pressure at 71.21 kPa after 6.0 months.

3.4. Stability Analysis Versus the Evolution of PWP based on LWL and HWL

Figures 10 to 13 shows a simple two-dimensional (2-D) finite element analysis (Slope/W) together with (Seep/W) that was performed to predict the existing safety factor *(SF)*. These resumes of extreme conditions were directly static (e.g., condition (infiltration of low-high rainfall) and additional condition of dynamic (e.g., local seismic potential)—fluid flow in steady-state to unsteady state conditions in determining PWP during water impounding. The pore water pressure (PWP) profile is governed by the net flow condition at the upper boundary, while the lower boundary typically assumes a state of hydrostatic pressure equilibrium.

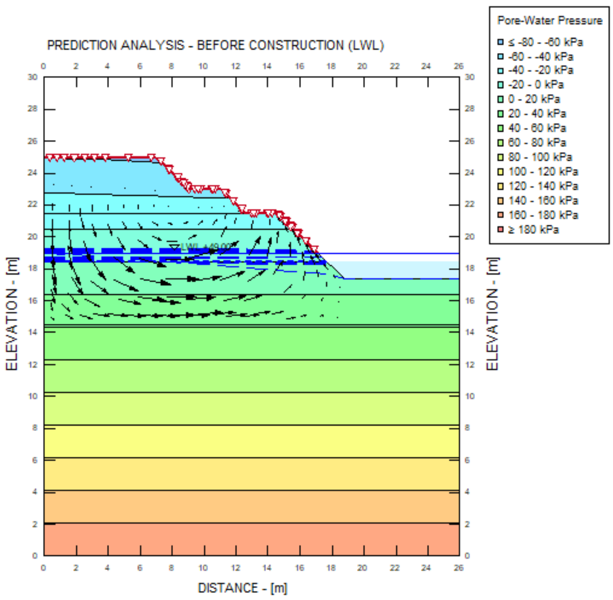

(a). Groundwater flow direction with low rainfall infiltration

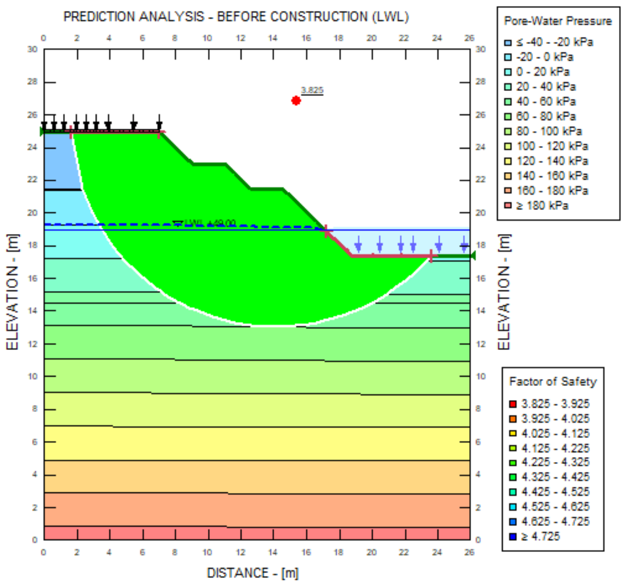

(b). Safety factor (SF: 3,825) of slope stability due to seepage

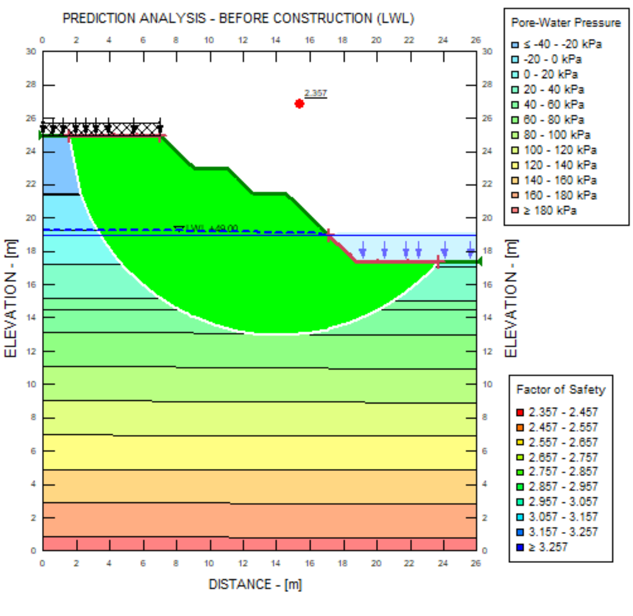

(c). Safety factor (SF: 2,357) of slope stability due to seepage + local seismic potential (due to earthquake)

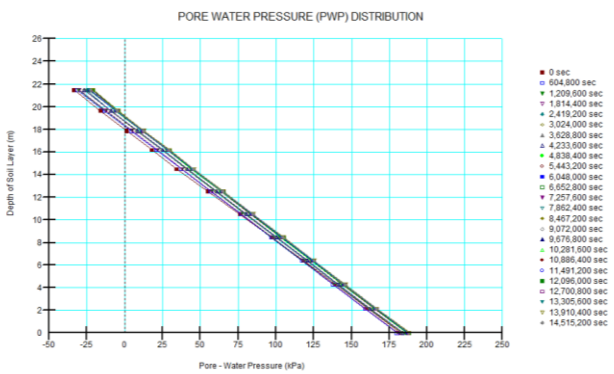

(d). Pore water pressure (PWP) distribution (At the body of dike)

Figure 10. Transition from normal consolidation (NC) to over-consolidation (OC) condition at LWL before water impounding (implication: cross-section area of soil pores-unchanged, etc.; and flow type-laminar only (steady state seepage condition).

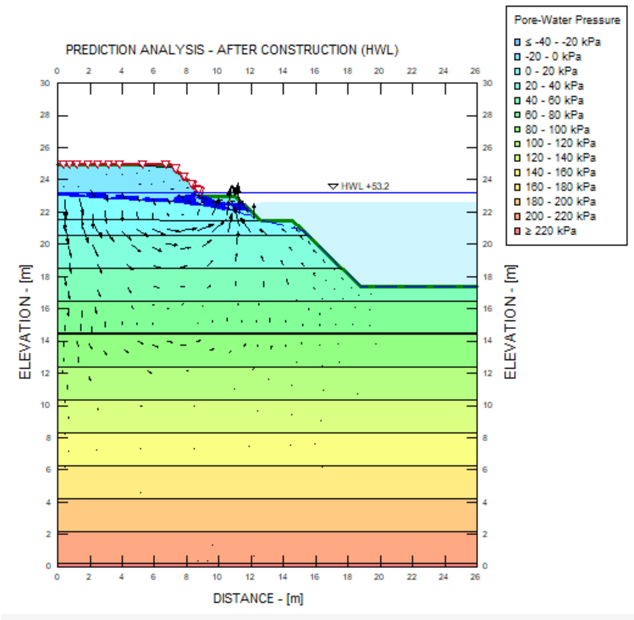

(a). Groundwater flow direction with high rainfall infiltration

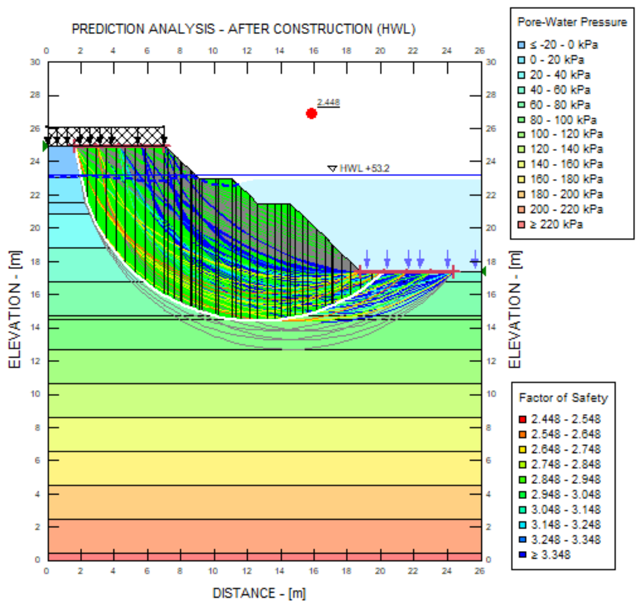

(b). Safety factor (SF: 2,448) of slope stability due to seepage

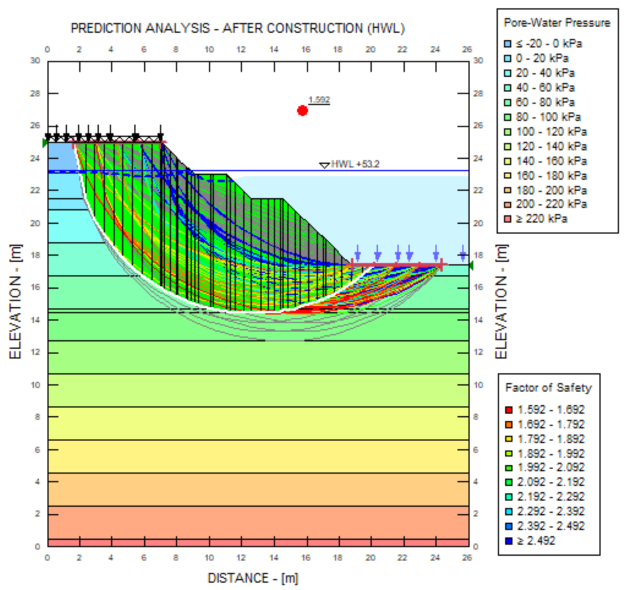

(c). Safety factor (SF: 1,592) of slope stability due to seepage and local seismic potential (due to earthquake)

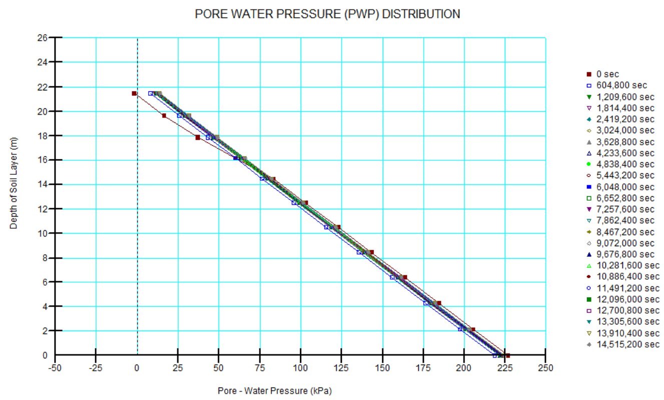

(d). Pore Water Pressure (PWP) Distribution (At the body of the dike)

Figure 11. Transition from normal consolidation (NC) to over-consolidation (OC) condition at LWL before water impounding (implication: cross-section area of soil pores-changed, etc.; flow type-laminar to transient (unsteady state seepage condition).

Figures 10 and 11 show the LWL at low rainfall and during fluctuation of LWL in low to high rainfall conditions. Both static conditions were selected because slope stability would be sensitive due to infiltration during low to high rainfall. Impact of PWP distribution on slope stability in Figure 10, PWP at the initial time (u0), and the clayey layer showed negative values in all cases. In case LWL at the prior fluctuation during steady state seepage condition (laminar flow type), rapid infiltration led to the phreatic surface forming at the slope toe away from the ground surface or, phreatic surface expanded locally around the toe, leading to a deep slide. Following this, the phreatic surface extended into the lower layer of the dike body rather than continuing to expand at the toe of the upper layer. This likely occurred due to the accumulated rainwater drainage from the slope failure in the ground surface. Changes of PWP in positive value occurred in the lower clayey layer, followed by the increasing stability or *(SF)* value [53].

Figure 11 shows the fluctuation during unsteady seepage conditions (flow transition from laminar to transient); a larger phreatic area will occur due to the higher rainfall intensity with a short duration. During short rainfall, the saturation process is slightly increased, and positive PWP develops, causing the phreatic surface to expand to the slope surface at the upper layer, leading to the initial failure at the slope toe near the ground surface. After the failure, the positive of PWP is increased significantly at the lower layer while reducing the upper layer or near the ground surface of the dike body. When failure first happens at the base of the slope, it forms cracks and fractures, which facilitate the drainage of water accumulated near the base or at the surface layer, lowering the pore water pressure (PWP) at the surface. This also changes the drainage pathways, allowing rainwater to penetrate deeper into the clay layers. Each scenario produces distinct outcomes, highlighting the intricate relationship between soil characteristics and the PWP in determining the safety factor (SF).

During dynamic conditions due to earthquake potential in a short time history, when the soil permeability in (OC) condition is very low, as shown in Figures 10 and 11, the dynamic PWP is much greater and is essentially symmetrical about the time of maximum load application [54, 55]. This is consistent with the permeability of the soil being so low that there is no opportunity for excess pore pressure dissipation when the load is applied. As the permeability is increased, the maximum induced PWP reduces, with a negative pore pressure being developed ahead of the moving load [56]. This is consistent with reducing the time available for PWP dissipation during dynamic loading [57]. In a saturated soil of a particular stiffness, the dynamic load and the *(k)* parameter determine the extent to which excess PWP builds up during the local seismic passage at any given depth. For short time histories, the soil behaves as highly permeable, with minimal excess pore pressure development. However, when the saturated soil layer is deeper, farther from the surface, or closer to the zero-pore-pressure boundary, this depth has only a limited effect on the excess pore pressure response across the range of soil stiffnesses being analyzed. Seepage and local seismic potential will significantly reduce the safety factor (SF).

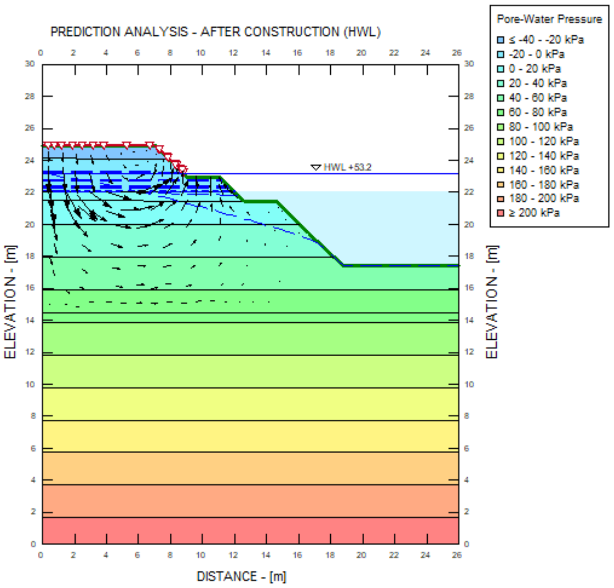

(a). Groundwater flow direction with high rainfall infiltration

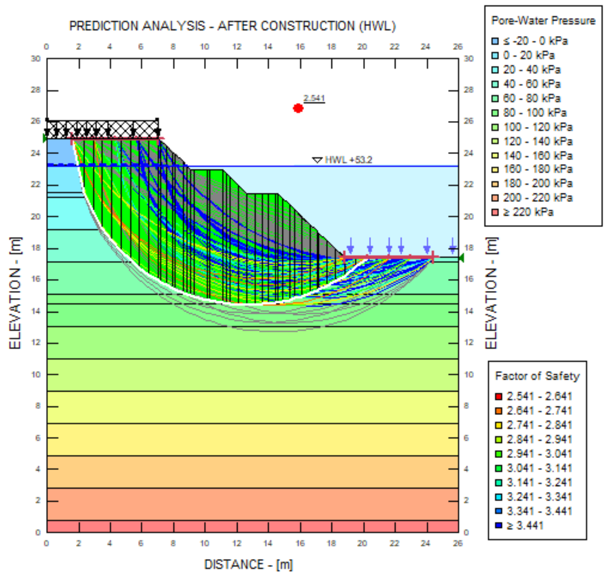

(b). Safety factor (SF: 2,541) of slope stability due to seepage

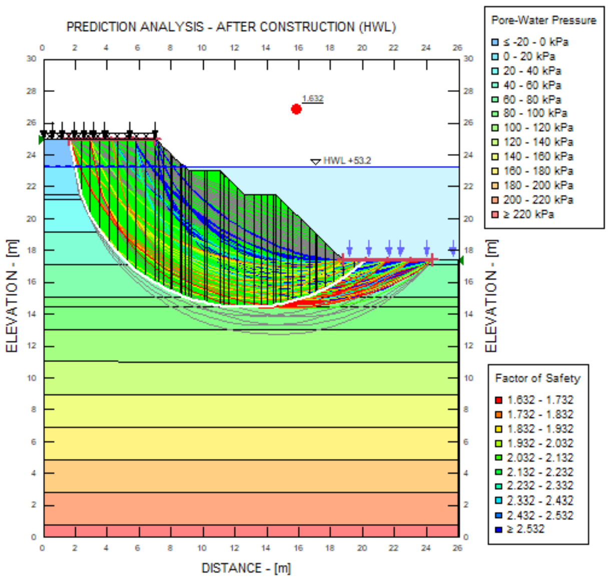

(c) Safety factor (SF: 1,632) of slope stability due to seepage and local seismic potential (due to earthquake)

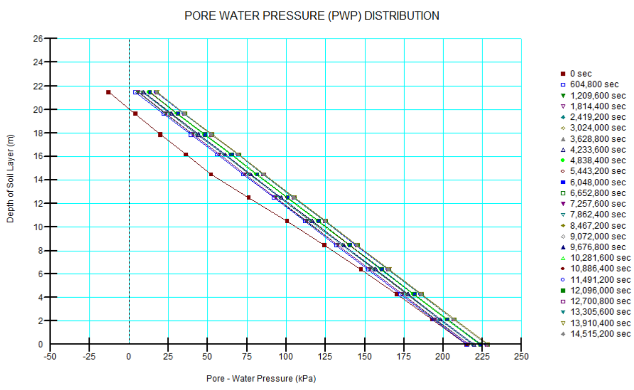

(d) Pore Water Pressure (PWP) distribution (at the body of the dike)

Figure 12. Over-consolidation (OC) condition at HWL after water impounding (implication: cross-section area of soil pores-unchanged, etc.; flow type-laminar only (steady state seepage condition)

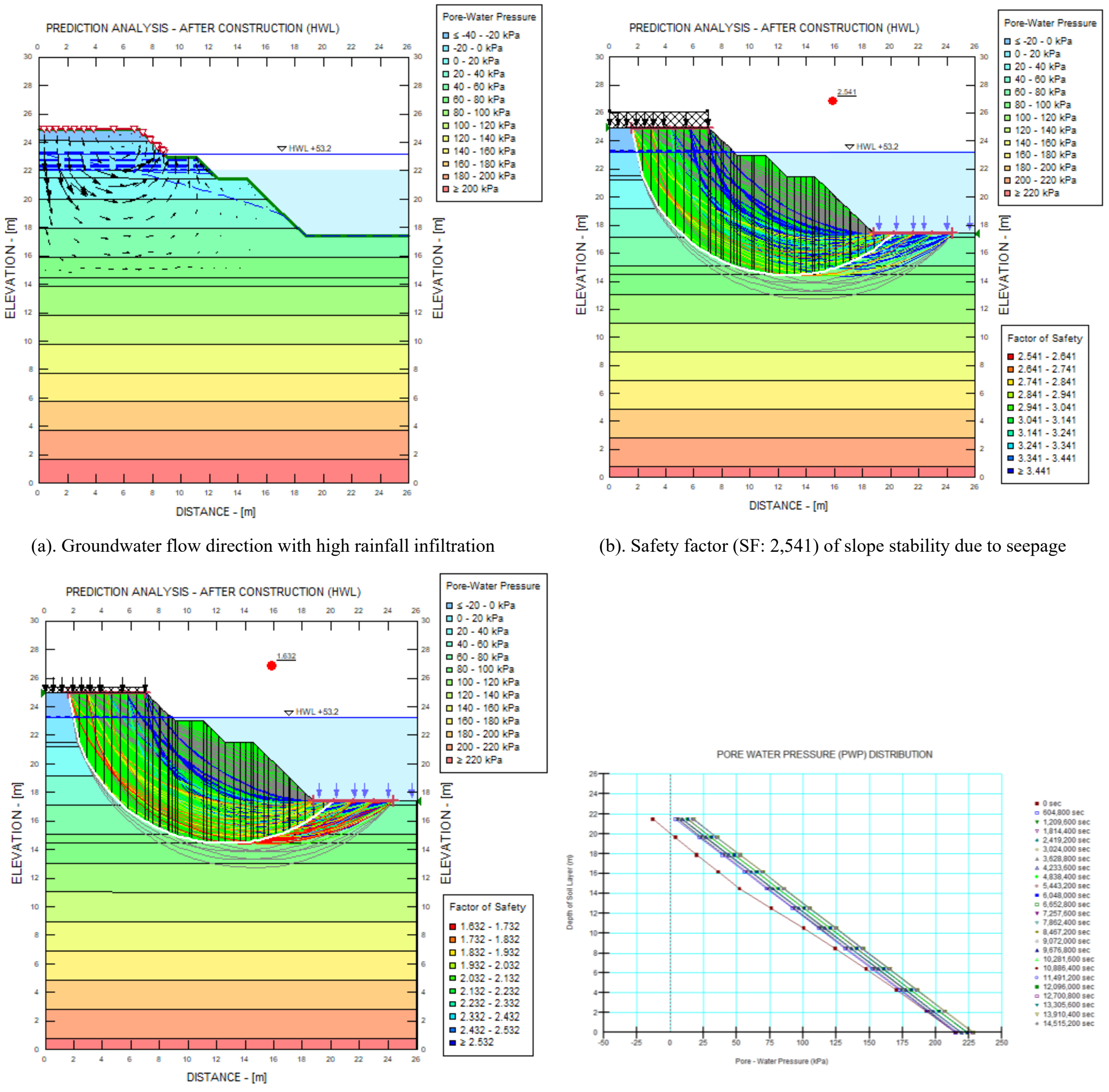

(a). Groundwater flow direction with high rainfall infiltration

(b). Safety factor (SF: 2,541) of slope stability due to seepage

(c) Safety Factor (SF: 1,632) of slope stability due to seepage and local seismic potential (due to earthquake)

(d) Pore water pressure (PWP) distribution (at the body of the dike)

Figure 13. Over-consolidation (OC) condition at HWL after water impounding (implication: cross-section area of soil pores-changed, etc.; flow type-laminar to transient (unsteady seepage condition)

Figures 12 and 13, under static conditions at the HWL during steady seepage (laminar flow), revealed a significant expansion of the phreatic surface and crack formation at the slope crest. This was likely caused by lower soil density and/or reduced soil stiffness. The failure mechanisms differed depending on the soil type, with a low likelihood of a complete slope failure. Instead, localized collapse at the slope toe was observed, suggesting that the upper clay layer could trigger more extensive shortcomings in the lower layers during prolonged rainfall events. In all cases for (OC) condition, the cross-section area of soil pores is unchanged and in steady-state seepage condition (e.g., laminar flow type), PWP will be dissipated smoothly with water infiltration and has a limited influence on slope stability, but the safety factor *(SF)* will be reduced.

In dynamic conditions, PWP is the primary factor that triggers slope failures where the (SF) is closing at 1.0; it is a notable influence in conditions of low weight volume of soil under high rainfall intensity. In this case, the localized slope toe will tend to fail when the phreatic surface appears on the slope surface as long as the rainfall duration. The positive distribution of PWP is more enlarged than that in the other two cases, as shown in Figures 10 and 11. Unlike the other two cases, the phreatic surface expanded to the upper part of the slope. This may be due to the lower volume of the clayey layer, and the HWL is a trigger of the increasing PWP besides the occurrence of backflow from the reservoir direction or unsteady seepage condition. When there is a backflow from the reservoir, changes in the cross-section of the soil pores can be predicted. Consequently, due to the large positive of PWP, some cracks would appear at the slope crest, and the *(SF)* value will be reduced due to the change of stress-state dependence [58].

From all simulations using the (Seep/W) and (Slope/W), it can be noticeable that the critical depth with the highest PWP would occur at a depth of around 4.0 m to the toe of the slope [59]. These results are almost close to both prediction analyses using the oedometer data in (1-D) for one and double-layer analysis, which were obtained around 3.75 m in a similar direction. Slip surfaces can occur at the highest elevation of PWP due to LWL and HWL conditions. Variations of external and internal change due to LWL and HWL can vary and/ or influence the magnitude of PWP dissipation in static and dynamic conditions. Comprehensive studies through laboratory modelling are required to demonstrate the change of PWP concerning the shift in stress-state-dependent parameters in natural conditions. The shift in stress-state dependence would be caused by altering the permeability coefficient (k) parameter in macroscopic terms. The shift can influence the change of (k) in the cross-section of soil pores, the sedimentation process at the soil pores during drying-wetting, etc. There are many shortcomings or limitations in assessing the magnitude measurements of PWP dissipation and *(k)* parameters during consolidation using the conventional oedometer data approach and the mathematical models, even if the resolution used numerical analysis.

3.5. Comparison of the Magnitude of Pore-Water Pressure (PWP) Distribution

Table 2 shows the variation of the magnitude of PWP through the prediction analysis using the oedometer data and the actual field measurement data from the piezometer instrumentations. The PWP dissipation using the oedometer data in the prediction analysis significantly differs at a depth of 6.0 m but has the same result at the 10.0 m depth because they have already reached the hydrostatic pressure. These values have a distinction of around 11% or slightly different if compared with the actual measurement based on the probabilistic method [60].

Table 2. Results of pore water pressure distribution

Depth of soil (m)	Amount of PWP based on actual measurement with VW piezometer (kPa)	Amount of PWP based on consolidation test with saturated 1D consolidation		Amount of PWP based on Finite Element Method Analysis			
				Transition NC to OC condition (LWL)		Over consolidation condition (HWL)	
		One layer (kPa)	Double layer (kPa)	Laminar only (kPa)	Laminar to Transient (kPa)	Laminar to Transient (kPa)	Laminar only (kPa)
6.0	81.20	100.05	111.75	55.30	47.90	95.75	69.45
10.0	89.05	93.80	93.80	74.95	68.15	114.0	92.20

By using the finite element analysis, the results could not be compared to each other because of the complexity analysis during the input soil parameter; there are unavailable data of the oedometer at (NC) or in transition condition from (NC) to (OC) when the beginning of prior water impounding [61]. However, it can be noticeable that a similar value is reached when the clayey soil layer at the dike is in (OC), and HWL conditions and the fluid flow is a transition seepage from steady state (e.g., laminar) to unsteady state (e.g., transient) at a depth of 6.0 and 10.0 m. Here, the acceptable condition is that the values of PWP at the (OC) are larger than the (NC) conditions. It can be implied that the increasing number of soil pores resulted in the decreasing permeability coefficient *(k)*.

This paper utilizes predicted and measured pore water pressure (PWP) data to evaluate the slope response to water impoundment or changes in the phreatic line, a scenario common in real-world conditions. Focusing on an ideal undrained dike slope, where excess pore water pressure forms at the base or toe, the study emphasizes the formation of a slip surface during the pre-failure phase before water impounding and the landslide kinematics after water is impounded in the reservoir. A parametric analysis explored how key parameters influence the slip surface's shape and location and the stress-state configuration of the clayey soil in the dike body, considering changes in PWP and permeability (k) as critical factors [62]. The findings indicate that while multiple parameters affect the slope response, excess pore pressure has the most significant impact. Finally, an equation proposed by earlier researchers for approximating PWP offers a valuable tool for assessing dike ponds' stability (safety factor) during their operational life.

4. Conclusion

This study presented the pore water pressure (PWP) assessment and stability analysis for a proposed dike pond before and after water impounding. High pore-water pressure occurring at the clay deposits can exceed the effective stress and reduce the safety factor of the dike body. The level of stability implemented in the safety factor (*SF)* satisfies all the conditions of stability analysis, such as steady and unsteady seepage, rainfall infiltration, and seismic loading. The increased PWP reduces the available soil shear strength. The groundwater table level does not control pore-water pressure distribution but may be affected by several factors. Predictions or actual measurements must be selected to determine the field's magnitude and distribution of pore-water pressure.

The primary role of PWP measurement is to reduce and control seepage flow through the reservoir body before and after water impoundment. The critical parameter in determining PWP is the coefficient of permeability (k) for each layer. Based on the basic theory of macroscopic analysis, the parameter (k) depends on the soil consolidation condition, whether normally consolidated (NC) or over-consolidated (OC). Volume changes or variations in the void ratio of clayey soil layers due to shifts in effective stress are evaluated using the coefficient of compressibility or the coefficient of consolidation, which are determined through the oedometer test in one-dimensional (1-D) prediction analysis. The length of the longest drainage path from initial to final conditions is essential for assessing PWP dissipation. Time and the final change in void ratio can be expressed as the consolidation ratio and/or the degree of percent consolidation. Ultimately, the induced excess PWP can be determined for each layer of clayey soil. In this study, slope stability analysis was conducted in conjunction with seepage analysis, considering fluctuations in PWP due to permeability (*k*) values less than or equal to £ 10^{-6} m/s in each layer of the dike body. Elevated PWP can reduce the stability of the dike or the safety factor (*SF*) in clay layers.

Furthermore, the study of slope stability of an earth dike on soft clayey soil examined the effect of changing soil properties on stability. In addition, the influence of soil parameters such as cohesion (*c*) and the angle of friction (*φ*) plays an essential role in the stability of the considered slope, as presented in this paper. The value of the safety factor (*SF*) decreases with the reduction of (*c*) and (*φ*) of the material. From seepage and stability simulation analysis, the results indicated that the (*SF*) ranges between 2.0 and 4.0 before and after water impounding, with the peak point of pore-water pressure (PWP) between 3.0 and 4.0 m.

5. Declarations

5.1. Author Contributions

Conceptualization, P.A.M.A. and M.F.R.H.; methodology, P.A.M.A., D.Y., and S.; software, D.Y., A.W.A., and M.A.A.; validation, A.S., M.A.M.R., and A.Z.; formal analysis, P.A.M.A., D.B.O., and M.A.A.; investigation, P.A.M.A., D.Y., S., A.W.A., and M.A.A.; resources, P.A.M.A. and M.F.R.H.; data curation, M.F.R.H., A.S., M.A.M.R., and A.Z.; writing—original draft preparation, P.AM.A. and M.F.R.H.; writing—review and editing, A.S., M.A.M.R., and A.Z.; visualization, D.Y., D.B.O., and M.A.A.; supervision, P.A.M.A. and M.F.R.H.; project administration, S. and A.W.A. All authors have read and agreed to the published version of the manuscript.

5.2. Data Availability Statement

The data presented in this study are available on request from the corresponding author.

5.3. Funding

The authors thank P3M Politeknik Negeri Jakarta for funding this research through the Research of Professor Acceleration (PAGB) grant with contract number 307/PL3.A.10/PT.00.06/2024.

5.4. Conflicts of Interest

The authors declare no conflict of interest.

6. References

[1] Sibiryakov, B., Leite, L. W. B., & Sibiriakov, E. (2021). Porosity, specific surface area and permeability in porous media. Journal of Applied Geophysics, 186, 104261. doi:10.1016/j.jappgeo.2021.104261.

[2] Residori, M., Mandal, S., Voigt, A., & Kurzthaler, C. (2025). Flow through porous media at the percolation transition. Physical Review Research, 7(1), 12032. doi:10.1103/PhysRevResearch.7.L012032.

[3] Ribolzi, O., Patin, J., Bresson, L. M., Latsachack, K. O., Mouche, E., Sengtaheuanghoung, O., Silvera, N., Thiébaux, J. P., & Valentin, C. (2011). Impact of slope gradient on soil surface features and infiltration on steep slopes in northern Laos. Geomorphology, 127(1–2), 53–63. doi:10.1016/j.geomorph.2010.12.004.

[4] Ventini, R., Dodaro, E., Gragnano, C. G., Giretti, D., & Pirone, M. (2021). Experimental and numerical investigations of a river embankment model under transient seepage conditions. Geosciences (Switzerland), 11(5), 192. doi:10.3390/geosciences11050192.

[5] Yun, S. K., Kim, J., Im, E. S., & Kang, G. (2022). Behavior of Porewater Pressures in an Earth Dam by Principal Component Analysis. Water (Switzerland), 14(4), 672. doi:10.3390/w14040672.

[6] Seyed-Kolbadi, S. M., Hariri-Ardebili, M. A., Mirtaheri, M., & Pourkamali-Anaraki, F. (2020). Instrumented health monitoring of an earth dam. Infrastructures, 5(3), 26. doi:10.3390/infrastructures5030026.

[7] Liu, W., & Zhao, Y. (2019). Research on the pore water pressure of submerged dike structure. IOP Conference Series: Earth and Environmental Science, 358(2), 22019. doi:10.1088/1755-1315/358/2/022019.

[8] Robertson, P. K. (2009). Interpretation of cone penetration tests — a unified approach. Canadian Geotechnical Journal, 46(11), 1337–1355. doi:10.1139/t09-065.

[9] Chang, W. J., Chou, S. H., Huang, H. P., & Chao, C. Y. (2021). Development and verification of coupled hydro-mechanical analysis for rainfall-induced shallow landslides. Engineering Geology, 293, 106337. doi:10.1016/j.enggeo.2021.106337.

[10] Al-Omari, A. A., Shatnawi, N. N., Shbeeb, N. I., Istrati, D., Lagaros, N. D., & Abdalla, K. M. (2024). Utilizing Remote Sensing and GIS Techniques for Flood Hazard Mapping and Risk Assessment. Civil Engineering Journal, 10(5), 1423–1436. doi:10.28991/CEJ-2024-010-05-05.

[11] Hasan, M. F. R., Susilo, A., Suryo, E. A., Agung, P. A. M., Idmi, M. H., Suaidi, D. A., & Aprilia, F. (2024). Mapping of Landslide Potential in Payung, Batu City, Indonesia, Using Global Gravity Model Plus (GGMplus) Data as Landslide Mitigation. Iraqi Geological Journal, 57(1), 159–168. doi:10.46717/igj.57.1A.13ms-2024-1-24.

[12] Koponen, A., Kataja, M., & Timonen, J. (1997). Permeability and effective porosity of porous media. Physical Review E, 56(3), 3319–3325. doi:10.1103/physreve.56.3319.

[13] Gui, M. W., & Wu, Y. M. (2014). Failure of soil under water infiltration condition. Engineering Geology, 181, 124–141. doi:10.1016/j.enggeo.2014.07.005.

[14] Turkandi, T., Sidarto, Agustiyanto, D. A., & Purbo, H. M. M. (1992). Geologic Map of Jakarta and Kepulauan Seribu Quadrangles, Jawa. Geological Research and Development Centre, Bandung, Indonesia.

[15] Huat, B. B., Ali, F. H., & Abdullah, A. (2005). Shear strength parameters of unsaturated tropical residual soils of various weathering grades. Electronic Journal of Geotechnical Engineering, 10(6), 1-16.

[16] Cevasco, A., Pepe, G., & Brandolini, P. (2014). The influences of geological and land use settings on shallow landslides triggered by an intense rainfall event in a coastal terraced environment. Bulletin of Engineering Geology and the Environment, 73(3), 859–875. doi:10.1007/s10064-013-0544-x.

[17] Merdassa, S., Garo, T., Chemeda, Y. C., Karuppannan, S., & Tesfaye, M. (2024). Engineering geological investigation of Gololcha dam for evaluation of leakage and abutment slope stability, Eastern Ethiopia. Scientific African, 26, 2381. doi:10.1016/j.sciaf.2024.e02381.

[18] Kabeta, W. F., Tamiru, M., Tsige, D., & Ware, H. (2023). An integrated geotechnical and geophysical investigation of landslide in Chira town, Ethiopia. Heliyon, 9(7), 17620. doi:10.1016/j.heliyon.2023.e17620.

[19] Durgunoglu, H. T., & Mitchell, J. K. (1973). Static penetration resistance of soils (No. SSL-SER-14-ISSUE-24). Contractor Report (CR), University of California, Berkeley, United States.

[20] Kumar, R., Bhargava, K., & Choudhury, D. (2016). Estimation of Engineering Properties of Soils from Field SPT Using Random Number Generation. INAE Letters, 1(3–4), 77–84. doi:10.1007/s41403-016-0012-6.

[21] Robertson, P. K., & Cabal, K. L. (2010). Estimating soil unit weight from CPT. 2nd International symposium on cone penetration testing. 9-11 May, 2010, Huntington Beach, United States.

[22] Agung, P. A. M., Sultan, R., Idris, M., Sudjianto, A. T., Ahmad, M. A., & Hasan, M. F. R. (2023). Probabilistic of in Situ Seismic Soil Liquefaction Potential Based on CPT-Data in Central Jakarta, Indonesia. International Journal of Sustainable Construction Engineering and Technology, 14(1), 241–248. doi:10.30880/ijscet.2023.14.01.021.

[23] Zhou, J., & Qin, C. (2022). Stability analysis of unsaturated soil slopes under reservoir drawdown and rainfall conditions: steady and transient state analysis. Computers and Geotechnics, 142, 104541. doi:10.1016/j.compgeo.2021.104541.

[24] Balasubramaniam, A. S., & Brenner, R. P. (1981). Consolidation and Settlement of Soft Clay. Developments in Geotechnical Engineering, 479–566, Elsevier, Amsterdam, Netherlands. doi:10.1016/b978-0-444-41784-8.50010-1.

[25] Terzaghi, K., Peck, R. B., & Mesri, G. (1996). Soil mechanics in engineering practice. John Wiley & Sons, Hoboken, United States.

[26] Lee, P. K. K., Xie, K. H., & Cheung, Y. K. (1992). A study on one-dimensional consolidation of layered systems. International Journal for Numerical and Analytical Methods in Geomechanics, 16(11), 815–831. doi:10.1002/nag.1610161104.

[27] Ayub Khan, P., Madhav, M. R., & Saibaba Reddy, E. (2010). Consolidation of thick clay layer by radial flow - non-linear theory. Geomechanics and Engineering, 2(2), 157–160. doi:10.12989/gae.2010.2.2.157.

[28] Ying, H., Zhang, L., Xie, K., & Huang, D. (2015). Pore Pressure Response to Groundwater Fluctuations in Saturated Double-Layered Soil. Mathematical Problems in Engineering, 2015, 389089. doi:10.1155/2015/389089.

[29] ASTM D2435-04. (2011). Standard Test Methods for One-Dimensional Consolidation Properties of Soils Using Incremental Loading. ASTM International, Pennsylvania, United States. doi:10.1520/D2435-04.

[30] Taylor, D. W. (1984). Fundamentals of soil mechanics. John Wiley & Sons, Inc., New York, United States.

[31] Francesco, R. Di. (2013). Exact Solution of Terzaghi's Consolidation Equation and Extension to Two/Three-Dimensional Cases. Applied Mathematics, 04(04), 713–717. doi:10.4236/am.2013.44099.

[32] Al Siaede, R. S. (2019). A practical geotechnical analysis of in situ stress variations and hydraulic stability of small weirs using SEEP/W and SIGMA/W simulation. Iraqi Journal of Science, 60(11), 2457–2467. doi:10.24996/ijs.2019.60.11.16.

[33] Krishnan, A., & Kolathayar, S. (2020). Stability Analysis of Dike to Impound Freshwater in Brackish Water Estuarine Environment. The Open Construction and Building Technology Journal, 14(1), 139–149. doi:10.2174/1874836802014010139.

[34] Wu, L., Huang, R., & Li, X. (2020). Hydro-mechanical Analysis of Rainfall-Induced Landslides. Springer Singapore. doi:10.1007/978-981-15-0761-8.

[35] SNI 8460. (2017). Geotechnical design requirements. Badan Standardisasi Nasional, Jakarta, Indonesia. (In Indonesian).

[36] Pagano, L., Fontanella, E., Sica, S., & Desideri, A. (2010). Pore water pressure measurements in the interpretation of the hydraulic behaviour of two earth dams. Soils and Foundations, 50(2), 295–307. doi:10.3208/sandf.50.295.

[37] Pradiptia, A., Agung, P. A. M., Pramusandi, S., Hasan, M. F. R., Suripto, Zainorabidin, A. Bin, & Ahmad, M. A. (2023). In-Situ Stabilization Analyses of Peaty Clay Soil Layers using Solid Waste from of Biomass Power Plant. International Journal of Design & Nature and Ecodynamics, 18(6), 1299–1313. doi:10.18280/ijdne.180603.

[38] Lovisa, J., Read, W., & Sivakugan, N. (2010). Consolidation Behavior of Soils Subjected to Asymmetric Initial Excess Pore Pressure Distributions. International Journal of Geomechanics, 10(5), 181–189. doi:10.1061/(asce)gm.1943-5622.0000061.

[39] Wang, L., & Chai, J. (2024). Time Series Prediction of Pore Water Pressure on Earth Dam Slopes Based on Recurrent Neural Network. Proceedings of the 2024 8th International Conference on Civil Architecture and Structural Engineering (ICCASE 2024), 675–686. doi:10.2991/978-94-6463-449-5_66.

[40] Parthasarathy, C. R., Sitharam, T. G., & Kolathayar, S. (2019). Geotechnical considerations for the concept of coastal reservoir at Mangaluru to impound the flood waters of Netravati River. Marine Georesources & Geotechnology, 37(2), 236–244. doi:10.1080/1064119X.2018.1430194.

[41] Dubey, R. P., Ghosh, A., Mitra, T., Choudhuri, B., Ghosh, S. N., & Khatun, S. (2017). Stability Analysis of River Dyke in Estuarine Environment. Indian Geotechnical Journal, 47(3), 349–363. doi:10.1007/s40098-017-0221-2.

[42] Rezaei, M., Ajalloeian, R., & Ghafoori, M. (2012). Geotechnical Properties of Problematic Soils Emphasis on Collapsible Cases. International Journal of Geosciences, 3(1), 105–110. doi:10.4236/ijg.2012.31012.

[43] Chien-Yuan, C., Tien-Chien, C., Fan-Chieh, Y., & Sheng-Chi, L. (2005). Analysis of time-varying rainfall infiltration induced landslide. Environmental Geology, 48(4–5), 466–479. doi:10.1007/s00254-005-1289-z.

[44] Ng, C. W. W., & Pang, Y. W. (2000). Influence of Stress State on Soil-Water Characteristics and Slope Stability. Journal of Geotechnical and Geoenvironmental Engineering, 126(2), 157–166. doi:10.1061/(asce)1090-0241(2000)126:2(157).

[45] Wu, L. Z., Zhu, S. R., & Peng, J. (2020). Application of the Chebyshev spectral method to the simulation of groundwater flow and rainfall-induced landslides. Applied Mathematical Modelling, 80, 408–425. doi:10.1016/j.apm.2019.11.043.

[46] Lei, H., Feng, S., & Jiang, Y. (2018). Geotechnical characteristics and consolidation properties of Tianjin marine clay. Geomechanics and Engineering, 16(2), 125–140. doi:10.12989/gae.2018.16.2.125.

[47] Baligh, M. M., & Levadoux, J. N. (1980). Pore pressure dissipation after cone penetration. Sea Grant College Program Massachusetts Institute of Technology, Cambridge, Massachusetts, United States.

[48] Martinez, A., & Stutz, H. H. (2024). Evolution of excess pore water pressure in undrained clay-structure interface shear tests. E3S Web of Conferences, 544, 1025. doi:10.1051/e3sconf/202454401025.

[49] Song, C., Bekele, B., & Silvey, A. (2019). Pore Pressure Responses of Overconsolidated Soils in a Partially Drained Piezocone Penetration Test. Journal of Engineering Mechanics, 145(4), 4019017. doi:10.1061/(asce)em.1943-7889.0001594.

[50] Fredlund, D. G., Rahardjo, H., Rahardjo, H., & Fredlund, M. D. (2012). Unsaturated Soil Mechanics in Engineering Practice. Wiley, Hoboken, United states.

[51] Wang, J., Li, S., Li, L., Song, S., Lin, P., & Ba, X. (2019). Simulated of flow in a three-dimensional porous structure by using the IB-SEM system. Geomechanics and Engineering, 18(6), 651–659. doi:10.12989/gae.2019.18.6.651.

[52] Simonsen, T. R., & Sorensen, K. K. (2017, September). Field measurements of pore-water pressure changes in a stiff fissured very high plasticity Palaeogene clay during excavation and pile driving. Proceedings of the 19th International Conference on Soil Mechanics and Geotechnical Engineering, Seoul, South Korea.

[53] Agung, P. A. M., Hasan, M. F. R., Baidhowy, M. S., Susilo, A., Suryo, E. A., Pramusandi, S., Adinegara, A. W., & Pradiptiya, A. (2025). Soil Shear Strength Analysis to Determine Landslide Potential Based on UU Triaxial Test. IOP Conference Series: Earth and Environmental Science, 1439(1), 12002. doi:10.1088/1755-1315/1439/1/012002.

[54] Agung, P. A. M., Ahmad, M. A., & Hasan, M. F. R. (2022). Probability Liquefaction on Silty Sand Layer on Central Jakarta. International Journal of Integrated Engineering, 14(9), 48–55. doi:10.30880/ijie.2022.14.09.007.

[55] Agung, P. A. M., & Ahmad, M. A. (2014). Potential Liquefaction Of Loose Sand Lenses: Case Study in Surabaya East Coastal Plain, Indonesia. International Journal of Integrated Engineering, 6(2), 1-10.

[56] Bian, X., Hu, J., Thompson, D., & Powrie, W. (2019). Pore pressure generation in a poro-elastic soil under moving train loads. Soil Dynamics and Earthquake Engineering, 125, 105711. doi:10.1016/j.soildyn.2019.105711.

[57] Mi, B., & Xiang, Y. (2020). Analysis of the limit support pressure of a shallow shield tunnel in sandy soil considering the influence of seepage. Symmetry, 12(6), 1023. doi:10.3390/SYM12061023.

[58] Tschuschke, W., Gogolik, S., Wrózynska, M., Kroll, M., & Stefanek, P. (2020). The application of the seismic cone penetration test (SCPTU) in tailingswater conditions monitoring. Water (Switzerland), 12(3), 737. doi:10.3390/w12030737.

[59] Yang, R., Xiao, P., & Qi, S. (2019). Analysis of Slope Stability in Unsaturated Expansive Soil: A Case Study. Frontiers in Earth Science, 7, 292. doi:10.3389/feart.2019.00292.

[60] Li, K. S., & Lo, S.-C. R. (2020). Probabilistic Methods in Geotechnical Engineering. CRC Press, London, United Kingdom. doi:10.1201/9781003077749.

[61] Singh, A., Singh, D., & Chakraborty, M. (2022). Effect of various initial excess pore water pressure distributions on 1-D consolidation of clays. International Journal of Geotechnical Engineering, 16(1), 123–132. doi:10.1080/19386362.2021.1956183.

[62] Zhai, Q., Rahardjo, H., & Satyanaga, A. (2019). Estimation of air permeability function from soil-water characteristic curve. Canadian Geotechnical Journal, 56(4), 505–513. doi:10.1139/cgj-2017-0579.